

Formation of strain-induced martensite in austempered ductile iron

Srinivasmurthy Daber · P. Prasad Rao

Received: 21 June 2006 / Accepted: 14 December 2006 / Published online: 6 November 2007
© Springer Science+Business Media, LLC 2007

Abstract The present work has been taken up to study the influence of microstructure on the formation of martensite in austempered ductile iron. Ductile iron containing 1.5 wt.% nickel and 0.3 wt.% molybdenum was subjected to two types of austempering treatments. In the first, called as conventional austempering, the samples were austempered for 2 h at 300, 350 or 400 °C. In the second treatment, called as stepped austempering, the samples were initially austempered at 300 °C for 10, 20, 30, 45 or 60 min. These were subsequently austempered for 2 h at 400 °C. Tensile tests revealed considerable variation in the strain-hardening behaviour of the samples with different heat treatments. In the case of samples subjected to conventional austempering, it was found that strain-hardening exponent increased with increasing austempering temperature. In the case of samples subjected to stepped austempering, increased strain hardening was observed in samples subjected to short periods of first step austempering. Study of the microstructures revealed that increased strain hardening was associated with the formation of strain-induced martensite. There was a greater propensity for the formation of strain-induced martensite in the samples containing more of blocky austenite. Retained austenite in the form of fine films between sheaths of ferrite was relatively more stable. Studies revealed that the morphology, size and carbon content of the retained austenite were important parameters controlling their tendency to transform to martensite.

Introduction

Austempered ductile iron (ADI) consists of a unique microstructure, called as ausferrite, which consists of ferrite and high-carbon austenite. This is unlike austempered steel which exhibits bainitic microstructure consisting of ferrite and carbide [1, 2]. The high silicon content in the ductile iron is responsible for the absence of carbides in the ADI. The austenite formed during the austempering process is highly stable because of its high carbon content, which may be in the range of 1.6–2.0 wt.% depending on the heat treatment parameters. The microstructures may consist of 20–45 vol.% of high-carbon austenite. It is believed that the presence of large amount of austenite imparts unusual property combinations of high strength and high ductility to ADI due to the high strain hardening nature of the austenite [1–3].

It has also been reported that trip phenomenon may occur in ADI which may be beneficial in improving the toughness [4, 5]. With regard to trip phenomenon, an important factor is the stability of the austenite during deformation. Too low a stability or too high a stability may not give the advantage of strain-induced martensite in increasing the ductility. There may be an optimum amount of retained austenite that may lead to maximum ductility.

Several parameters influence the stability of the retained austenite during deformation [6]. These are the carbon content of the retained austenite [7–9], size [10–12] and morphology of the retained austenite [13, 14] and its distribution within the microstructure [15]. All these are microstructural features, and the microstructures are markedly influenced by the heat treatment parameters. However, the influence of the heat treatment parameters such as austenitising temperature, and austempering temperature and time has not been studied systematically.

S. Daber · P. Prasad Rao (✉)
Department of Metallurgical and Materials Engineering,
National Institute of Technology Karnataka, P.O. Srinivasnagar,
Surathkal 575025, Karnataka, India
e-mail: ppr@nitk.ac.in

Hence the present work has been taken up to study the influence of some of the heat treatment parameters such as the austempering temperature and time on the formation of martensite during plastic deformation of ADI.

Experimental work

Material

The ductile iron required for the investigation was prepared in the form of slabs of dimension 200 mm × 150 mm × 30 mm. The chemical composition in wt.% was as follows: C: 3.5, Si: 2.8, Mn: 0.3, S: 0.02, P: 0.02, Mg: 0.04, Cu: 0.5, Ni: 1.5, Mo: 0.3. Coupons of dimension 20 mm × 20 mm × 2 mm for microscopic studies and round tensile samples of diameter 6 mm and gauge length 30 mm were machined from the cast slabs.

Heat treatment

Two types of heat treatments were carried out in the present investigation. The first one, called hereafter as “conventional austempering”, consisted of austenitising the samples at 950 °C for 30 min followed by austempering at 300, 350 or 400 °C for 2 h. In the second austempering treatment, called hereafter as “stepped austempering”, the same austenitising conditions were followed as in the conventional austempering. This was followed by austempering at two different temperatures. The austenitised samples were first austempered at 300 °C for 10, 20, 30, 45 or 60 min and then transferred to a second furnace at 400 °C and maintained at that temperature for 2 h. The schematic of the heat treatments is shown in Fig. 1.

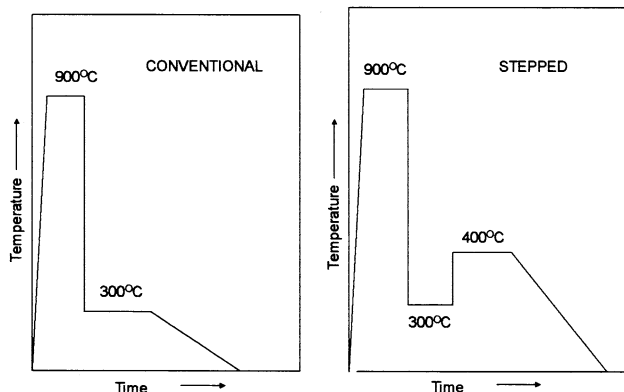


Fig. 1 Schematic of heat treatment schedules employed in the present investigation

All the austenitising treatments were done in muffle furnaces. The samples were tied with long nichrome wires for quick pull out from the furnace at the end of the austenitising treatment. The austempering treatments were carried out in salt bath furnaces. A mixture of sodium nitrate and sodium nitrite was used as the salt bath. The samples, which were relatively small compared to the salt bath capacity, were quickly transferred from the muffle furnace into the salt bath. The same wires were used in transferring the samples from the first salt bath to the second. Because of the small size of the sample, there was hardly any variation in the temperature of the salt bath. The time durations in the salt bath were counted from the moment the samples were introduced into the salt bath. The temperature was controlled within $\pm 1^\circ\text{C}$ of the set point.

Microstructural studies

Morphological features of the microstructures were studied using optical microscope after etching the samples with 3% nital. Quantitative information on the amount of retained austenite and its carbon content were obtained through X-ray diffraction on Jeol JDX 8P diffractometer. Diffraction studies were carried out using $\text{CuK}\alpha$ radiation, and scanning was done over the 2θ range of $40\text{--}50^\circ$ at a scan speed of 1°min^{-1} .

The volume fraction of the retained austenite was determined by the direct comparison method of Cullity [16] using integrated intensities of (110) peak of ferrite and (111) peak of austenite. Assuming that ferrite and austenite were the only matrix phases present, the ratios of integrated intensities of diffraction peaks from these phases can be written as

$$I_{\gamma(\text{hkl})}/I_{\alpha(\text{hkl})} = (R_{\gamma(\text{hkl})}/R_{\alpha(\text{hkl})}) \cdot (X_{\gamma}/X_{\alpha}) \quad (1)$$

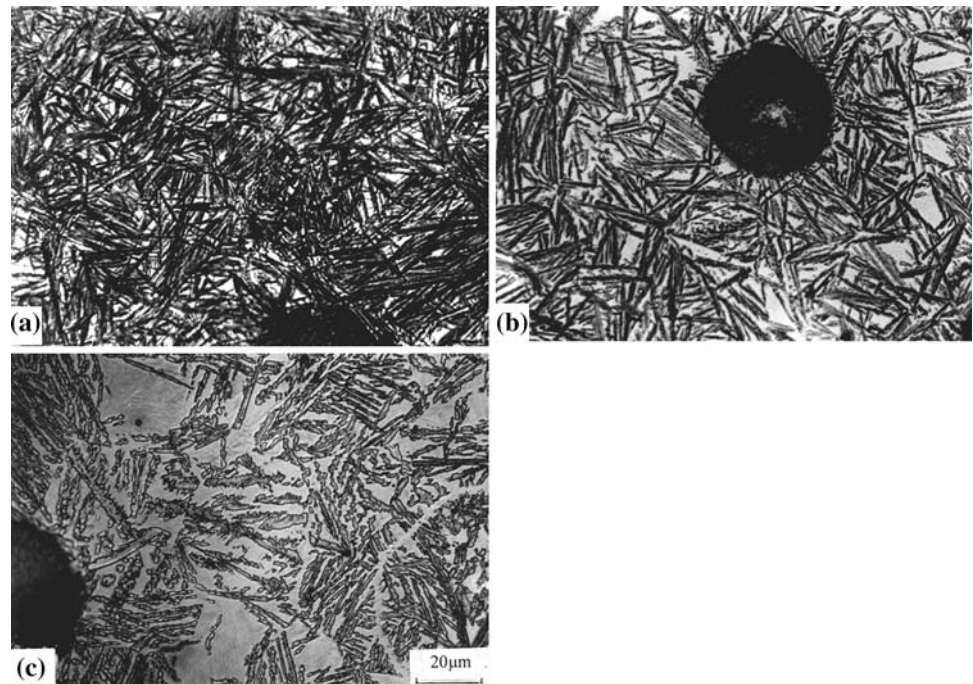
where $I_{\gamma(\text{hkl})}$ and $I_{\alpha(\text{hkl})}$ are the integrated intensities of a given (hkl) plane from the γ phase and the integrated intensity of a given (hkl) plane from the α phase respectively. X_{γ} and X_{α} are the volume fractions of retained austenite and ferrite respectively. The constants $R_{\gamma(\text{hkl})}$ and $R_{\alpha(\text{hkl})}$ are given by the following expression for each peak:

$$R = (1/v^2) [F^2 \cdot p \cdot LP] e^{-2m} \quad (2)$$

where v is the volume of the unit cell; F is the structure factor; p is the multiplicity factor; LP is the Lorentz polarization factor; and e^{-2m} is the temperature factor.

The lattice parameter of austenite increases with its carbon content. The following empirical relationship from the classical work of Roberts [17] is widely accepted:

Fig. 2 Microstructures of samples subjected to conventional austempering at (a) 300 °C, (b) 350 °C, and (c) 400 °C



$$a_{\gamma} = 0.3548 + 0.0044C_{\gamma} \quad (3)$$

where a_{γ} is the lattice parameter of austenite in nanometers and C_{γ} is its carbon content in wt.%. The Bragg angle obtained from the (111) peak of austenite was used in estimating the lattice parameter. The carbon content was then estimated using this value of the lattice parameter in the above equation.

In estimating the total carbon of the ausferrite it is assumed that all the carbon is present in the retained austenite, and that the ferrite is free of carbon. It is further assumed that the densities of ferrite, austenite and ausferrite are same. Now consider a unit volume of ausferrite. The volume of retained austenite in it will be X_{γ} . The mass of ausferrite and retained austenite will be ρ and $X_{\gamma} \cdot \rho$, respectively. The mass of carbon is given as $X_{\gamma} \cdot \rho \cdot C_{\gamma} / 100$. Therefore, the carbon content of the ausferrite in wt.% can be given as $(X_{\gamma} \cdot \rho \cdot C_{\gamma} / 100) \cdot 100 / \rho$. Thus the product $X_{\gamma} C_{\gamma}$ gives the carbon content of the ausferrite in wt.%.

Mechanical properties

Tensile tests were carried out on a floor model 10T Instron machine (model 4206) at a cross head speed of 1 mm min^{-1} . Three tests were carried out for each heat treatment, and the results reported are an average of these three tests. Yield strength, ultimate tensile strength and elongation to failure were estimated from the tensile tests.

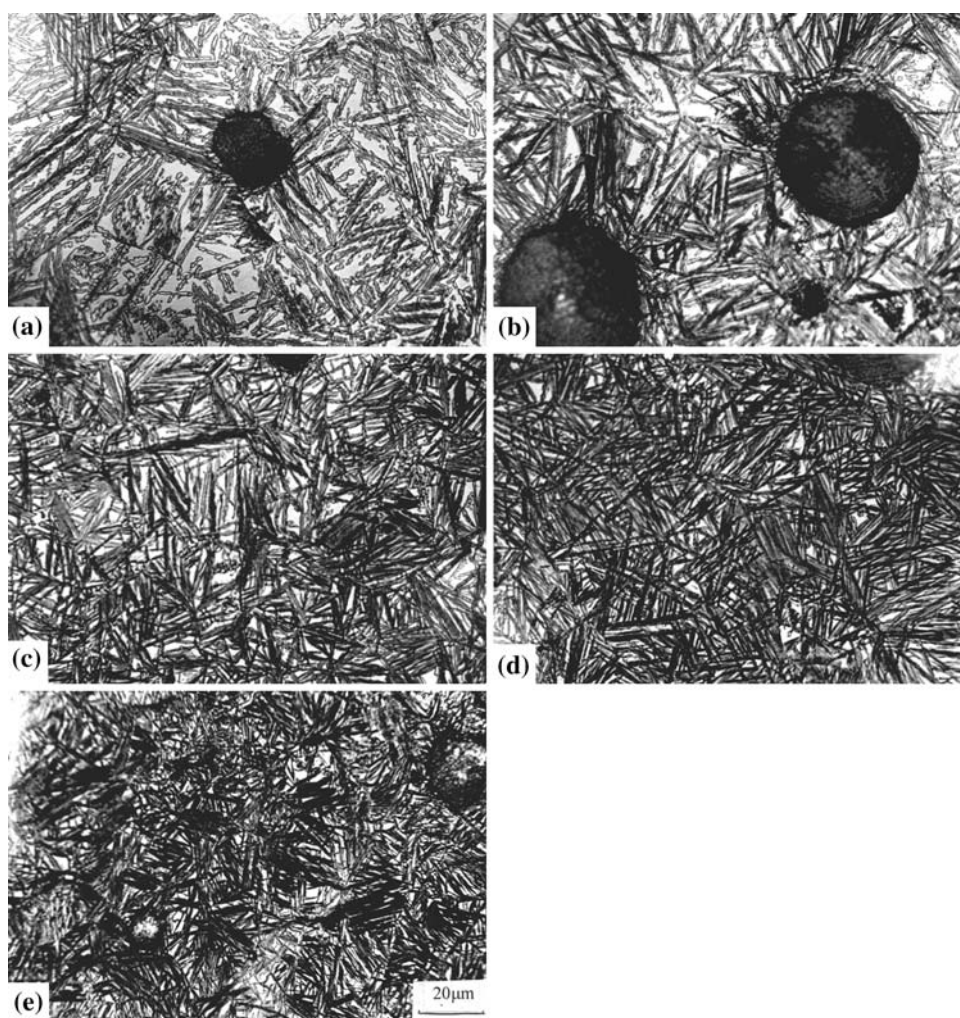
Results and discussion

Microstructural studies

On austempering at 300 °C, the samples exhibited a fine mixture of ferrite and austenite. As the austempering temperature was raised, the retained austenite content increased and the ferrite sheaths became broader. This can be observed in Fig. 2. While the austenite was present as fine slivers between the ferrite sheaths at 300 °C, it was present as blocky regions at 400 °C, well separating the ferrite sheaths from each other. These observations can be explained on the same basis as done by previous investigators [2, 3, 18, 19].

Stepped austempering resulted in a mixed microstructure consisting of both upper and lower ausferrites. The relative amounts of the two depended on the time of the first step austempering. As this time was increased, the relative amount of the lower ausferritic constituent increased. Figure 3 shows a typical set of microstructures resulting from stepped austempering. Figure 3a shows a sample in which the first step time was 10 min. The microstructure shows very broad sheaths of ferrite separated by broad areas of retained austenite. The microstructure looks very similar to that of a sample subjected to conventional austempering at 400 °C. Since the first step duration is very small, very small amount of lower ausferrite would have formed and the microstructure would be almost fully upper ausferrite. As the first step time was increased to 30 min, the amount of the lower ausferrite increased while that of the upper ausferrite decreased, as

Fig. 3 Microstructures of samples subjected to stepped austempering. First step times are (a) 10 min, (b) 20 min, (c) 30 min, (d) 45 min, and (e) 60 min



shown in Fig. 3b. As the first step time was increased further, the broad ferrite sheaths of the upper ausferrite progressively decreased, till, at 60 min of the first step time, the microstructure resembled that of a sample subjected to conventional austempering at 300 °C (see Fig. 3c). Existence of a composite microstructure, consisting of upper and lower ausferrite constituents, could be clearly seen in the samples with the first step times of 20, 30 and 45 min. Figure 4 shows one such microstructure, at a higher magnification. The sample was subjected to first step austempering of 20 min at 300 °C. Closely spaced sheaths of lower ausferrite are visible clearly, and are marked as 'b'. Upper ausferrite consisting of broader ferrite separated from each other by bulky austenite is visible at 'a'.

Quantitative information on the microstructures, such as the amount of the retained austenite, its carbon content and the total carbon content of the ausferrite, were obtained through X-ray diffraction. The influence of the austempering

temperature on the amount of the retained austenite and its carbon content is shown in Fig. 5. As the austempering temperature was increased, the amount of the retained austenite increased from 32 vol.% at 300 °C to 48 vol.% at 400 °C. However, its carbon content decreased from about 2.1 wt.% at 300 °C to about 1.7 wt.% at 400 °C. These results are in good agreement with those of earlier investigators [2, 3, 18, 19], and can be explained on the same basis. As the austempering temperature is raised diffusion of carbon from the regions transforming to ferrite to the surrounding austenite will be higher. This will lead to increasing stability of the austenite, and therefore to increasing amount of the retained austenite, as the austempering temperature is raised. In order to understand the decreasing carbon content with increasing austempering temperature, one has to look at the total carbon in the austenite, which is given by the product $X_\gamma C_\gamma$, where X_γ is the volume fraction of the retained austenite, and C_γ is its carbon content. This product can have a maximum value of C_{γ_0} , the

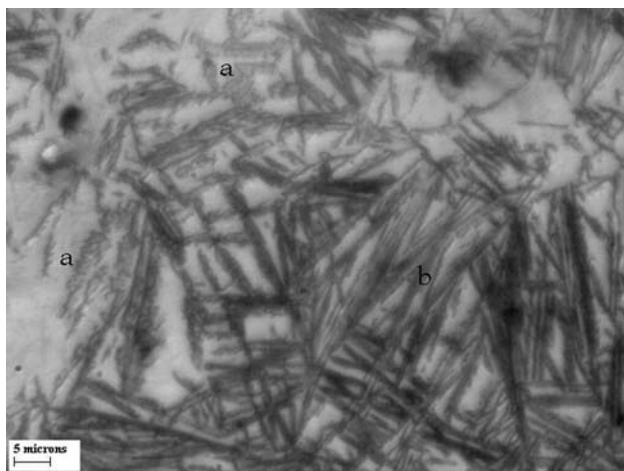


Fig. 4 Microstructure of sample subjected to stepped austempering, first step time of 20 min. ‘a’ indicates upper ausferrite region while ‘b’ indicates lower ausferrite region

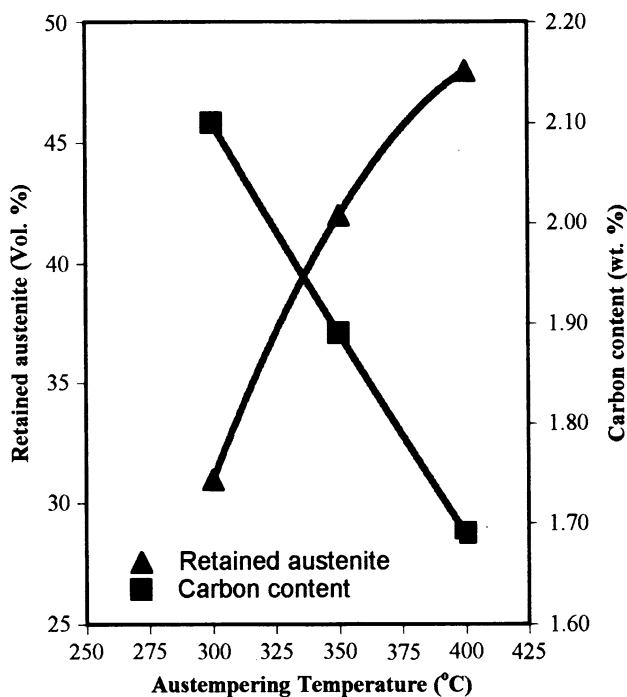


Fig. 5 Influence of the austempering temperature on the volume fraction of retained austenite and its carbon content during conventional austempering

initial carbon content of the austenite immediately after austenitising. The value of C_{γ_0} can be obtained from the following equation [20]:

$$C_{\gamma_0} = (T_{\gamma}/420) - 0.17(\text{Si}) - 0.95 \quad (4)$$

where T_{γ} is the austenitising temperature in degrees Celsius, and Si is the silicon content of the ductile iron in wt.%. Though the carbon content of the retained austenite is lower at higher austempering temperatures, the total

carbon will be higher. These values are 0.62, 0.76 and 0.79 at the three austempering temperatures of 300, 350 and 400 °C, respectively. It can be seen that the total carbon is almost equal to the maximum possible value as given by the Eq 4. Therefore, the lower carbon content of the retained austenite is due to the increased amount of retained austenite, and not because less carbon is finding its way into the retained austenite.

The quantitative values of the microstructural features were estimated in the samples subjected to stepped austempering also. Figure 6 shows the influence of the first step time on the retained austenite content and its carbon content. As the first step austempering time was increased, the retained austenite content decreased steadily from a value close to that of conventional austempering at 400 °C to that similar to conventional austempering at 300 °C. Similar trends were observed in the case of the carbon content of the retained austenite as well. These confirm the earlier conclusion drawn from the optical microscopic studies that, at the two extremes of stepped austempering, the samples are similar to those of conventional austempering, while for the intermediate durations of first step austempering, the samples exhibit a composite microstructure. As the first step time is increased, the microstructure changes from that characteristic of conventional austempering at 400 °C to that characteristic of conventional austempering at 300 °C.

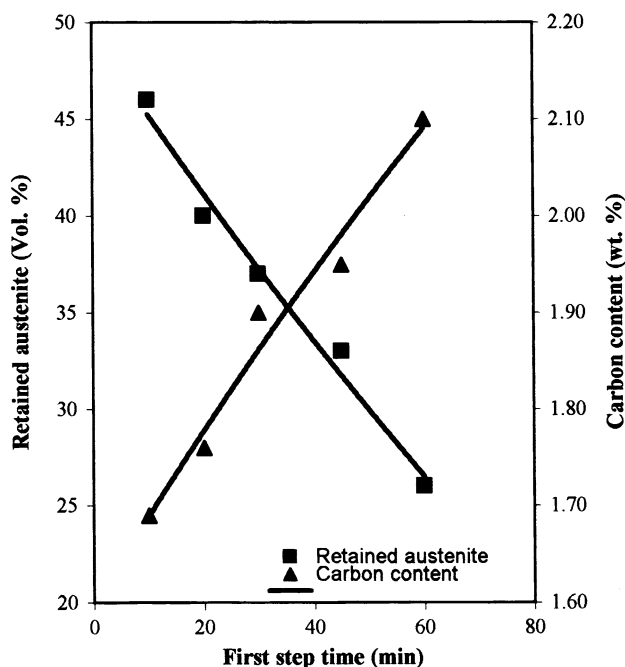


Fig. 6 Influence of first step time on the retained austenite content and its carbon content during stepped austempering

Mechanical properties

Mechanical properties are known to be a function of the microstructure. Since the microstructure of the ADI changes markedly with heat treatment, profound changes in the mechanical properties too can be expected with changes in heat treatment. Hardness and tensile properties, such as yield strength, ultimate tensile strength and elongation to failure together with strain hardening behaviour, were studied in detail under different heat treatment conditions to understand the influence of the heat treatment and the microstructure on them.

The tensile studies revealed that strength values were higher when austempered at 300 °C than at 400 °C. Ductility, as revealed by percentage elongation, showed the opposite effect. The results are presented in Fig. 7. The increasing strength with decreasing austempering temperature can be attributed to the finer microstructure and lower retained austenite content at the lower temperatures.

In order to understand completely the influence of the microstructure on the tensile behaviour, the strain-hardening nature under different heat treatment conditions was studied. In order to do this, it was assumed that the following relationship due to Holloman [21] is obeyed:

$$\sigma = K \cdot \varepsilon^n \quad (5)$$

where n is the strain-hardening coefficient and K is the strength factor. If the above relationship is obeyed, a plot of

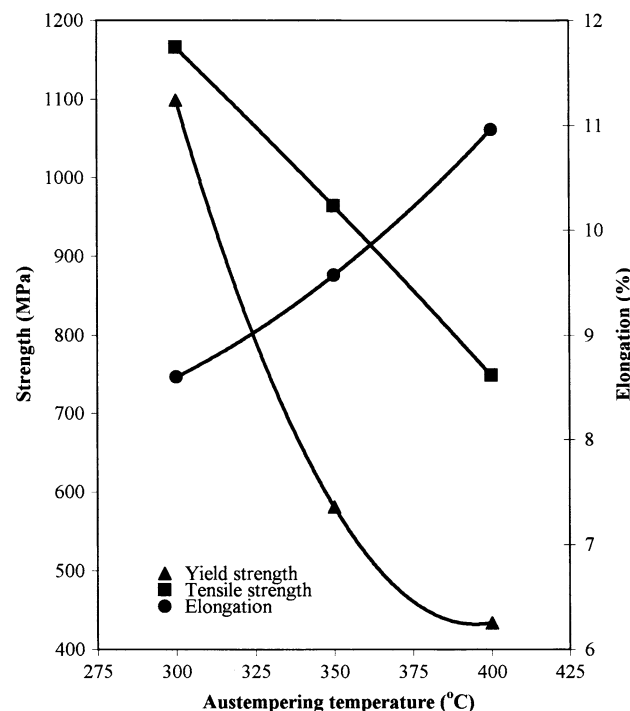


Fig. 7 Tensile properties of samples subjected to conventional austempering

In σ against $\ln \varepsilon$ should result in a straight line, the slope of which will give the strain-hardening exponent n . If there is a change in strain-hardening mechanism during the deformation process, the plot will show a change of slope. Figure 8 shows the plot of $\ln \sigma$ against $\ln \varepsilon$ at the three austempering temperatures of 300, 350 and 400 °C. The sample austempered at 300 °C shows a single straight line with an n value of 0.14. However, the sample austempered at 350 °C shows a change of slope, with n values of 0.14 and 0.18 for the two stages. A close examination of the plot for the sample austempered at 400 °C reveals that it is curved. This curvature indicates a continuous change in the strain-hardening behaviour from an early stage as the sample is strained. However, two straight lines are drawn through the data points as an approximation. From these the n values were taken as 0.17 and 0.21, respectively for the two stages.

Thus the above results indicate that there is no change in the strain-hardening behaviour of the samples austempered at 300 °C, when strained to fracture. However, the samples austempered at 400 °C do show pronounced increase in strain-hardening tendency as they are increasingly strained. This indicates that certain changes are taking place in the microstructure as the material is deformed. To understand this, the material adjacent to the fracture surface was examined by optical microscopy as well as X-ray diffraction. The fracture surface was ground, polished and etched to reveal the microstructure in an area severely deformed just prior to fracture. Figure 9a shows the microstructure

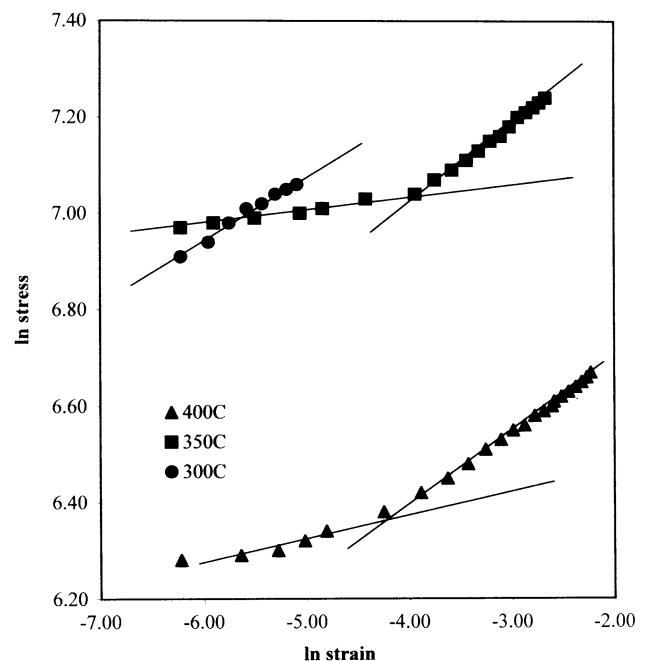


Fig. 8 Strain-hardening behaviour of samples subjected to conventional austempering

Fig. 9 Microstructures of fracture surfaces of samples subjected to conventional austempering: (a) 300 °C, (b) 350 °C, and (c) 400 °C. M indicates regions of martensite

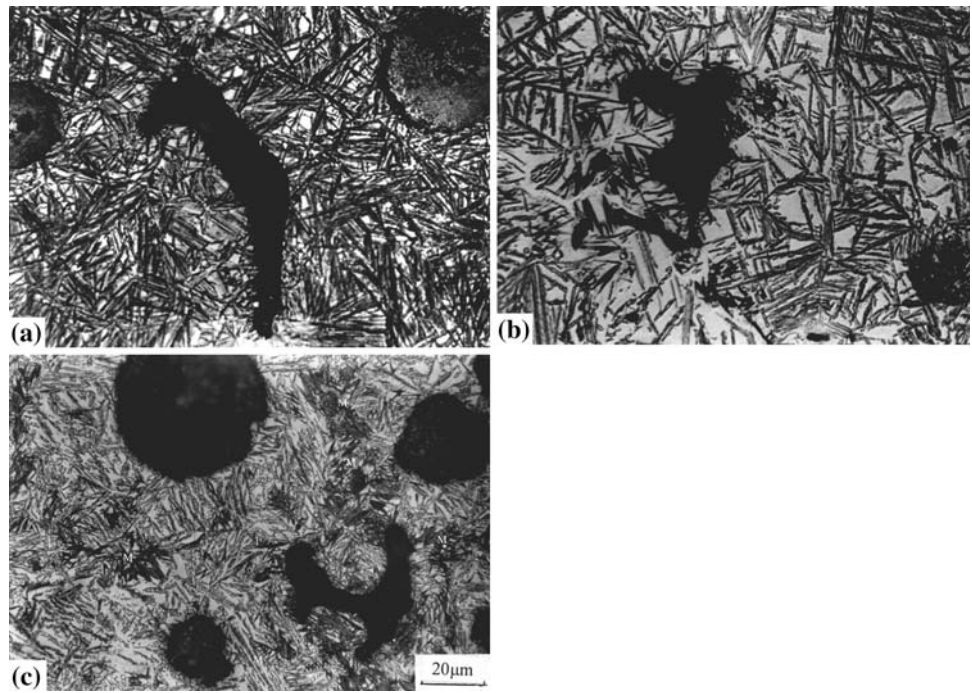
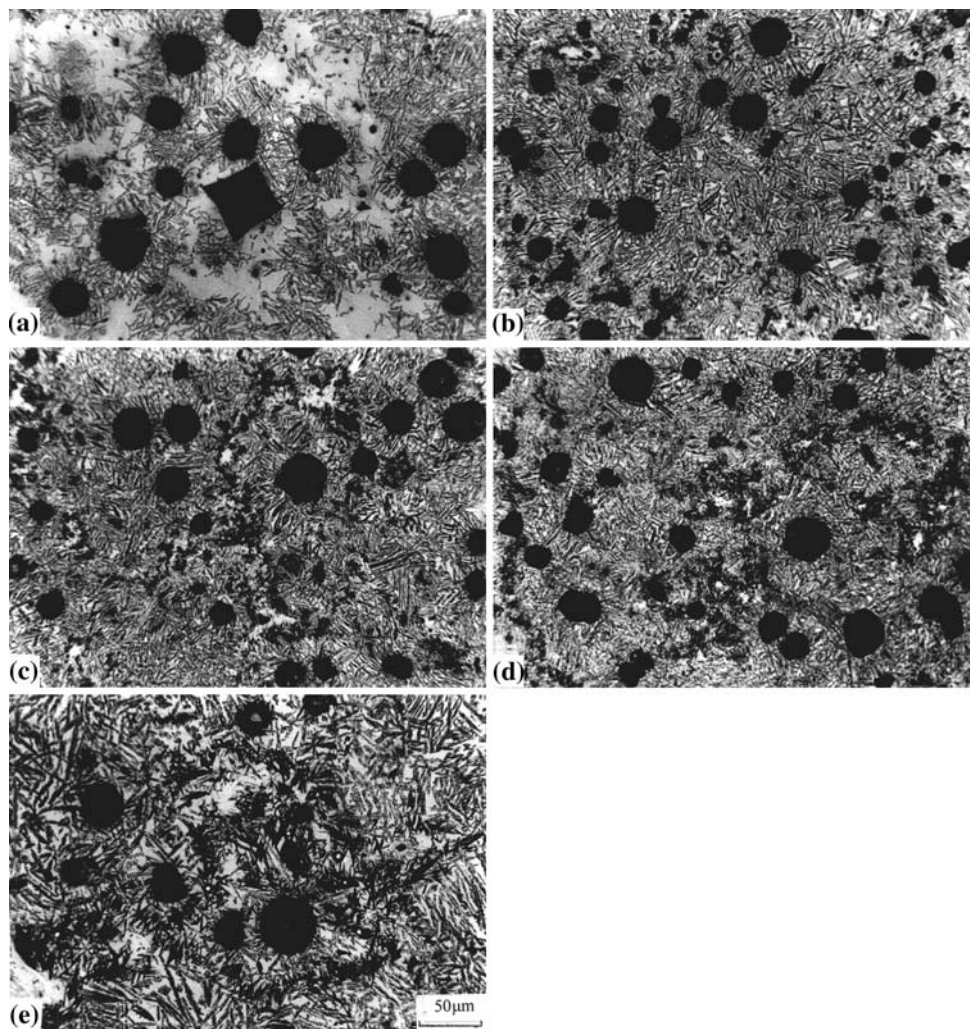


Fig. 10 Microstructures of samples subjected to conventional austempering at 400 °C and deformed by (a) 0%, (b) 3%, (c) 5%, (d) 7%, and (e) 9%



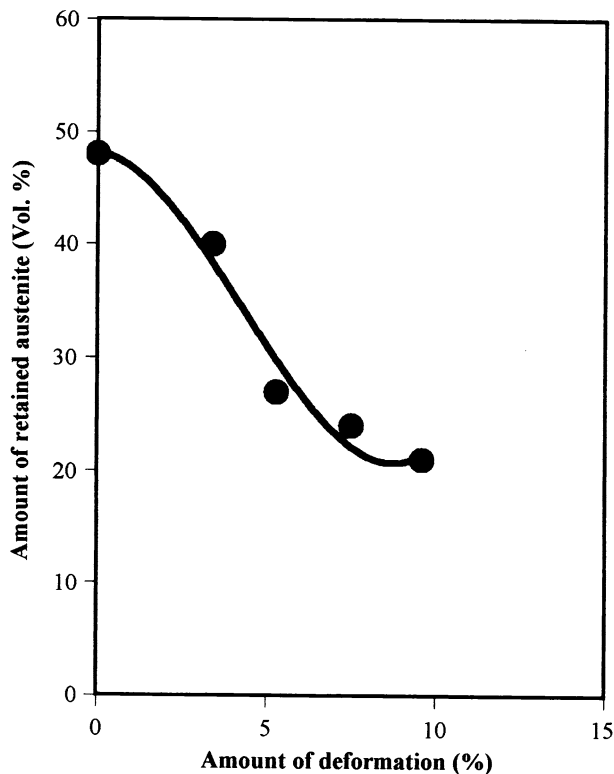


Fig. 11 Variation of retained austenite content with amount of deformation. Conventional austempering at 400 °C

adjacent to the fracture surface of the sample austempered at 300 °C. These are not different from those in Fig. 2a, of the undeformed samples under identical heat treatment conditions. Figure 9c shows the microstructure adjacent to the fracture surface of the sample austempered at 400 °C. This shows marked differences with those in Fig. 2c under identical heat treatment conditions. Considerable formation of martensite is observed, which is marked as M at several locations. These are the strain-induced martensite formed from the retained austenite during the deformation. Indeed, X-ray diffraction studies showed that the retained austenite content had dropped to 24 vol.% from the original values of 48 vol.%. In the samples austempered at 400 °C soft ductile austenite is being replaced by hard and brittle martensite which provides greater resistance to the movement of dislocations. This is the cause of increasing strain hardening in these samples. Strain-induced martensite formation is observed in the samples austempered at 400 °C, and not in those austempered at 300 °C. This may be attributed to the lower stability of the retained austenite in the former than in the latter. Carbon content of the retained austenite in the samples austempered at 400 °C was lower than that in the samples austempered at 300 °C as seen in Fig. 5. As indicated in Fig. 9b, and as revealed by microscopic and diffraction studies, the samples austempered at 350 °C showed a behaviour intermediate to

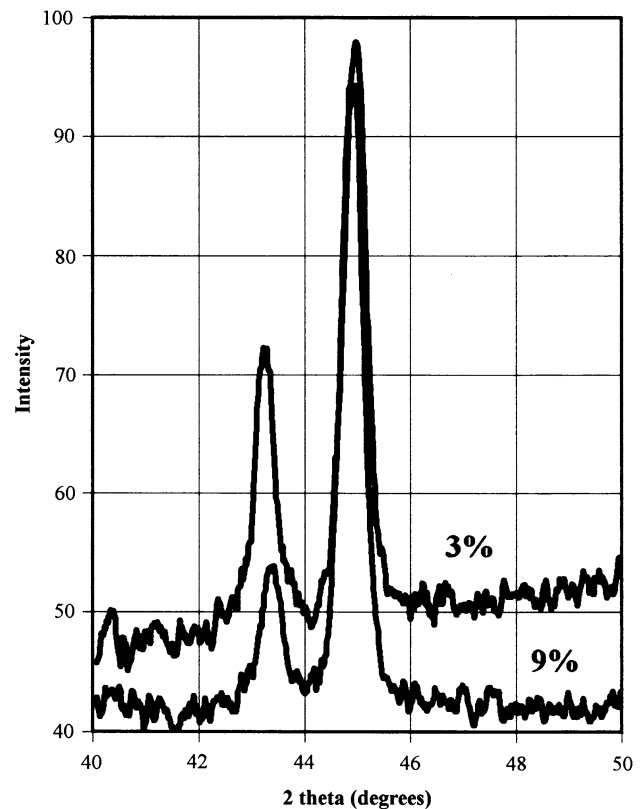


Fig. 12 X-ray diffraction profiles of samples after 3% and 9% deformation

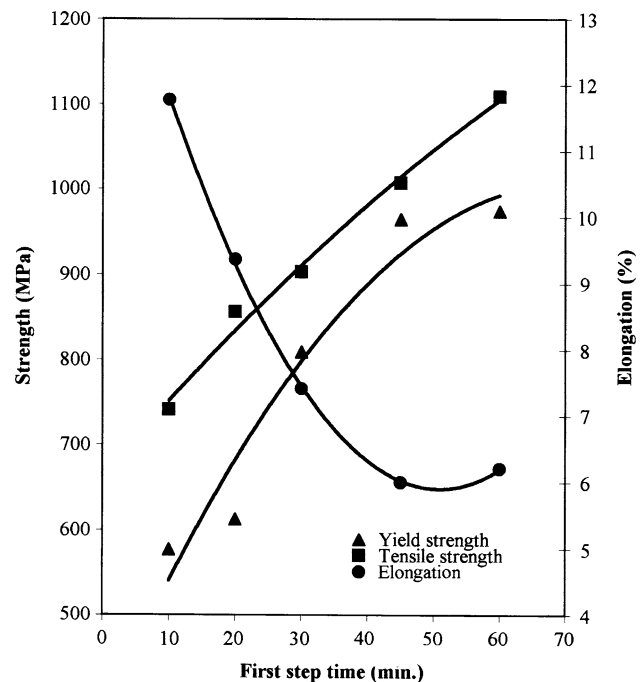
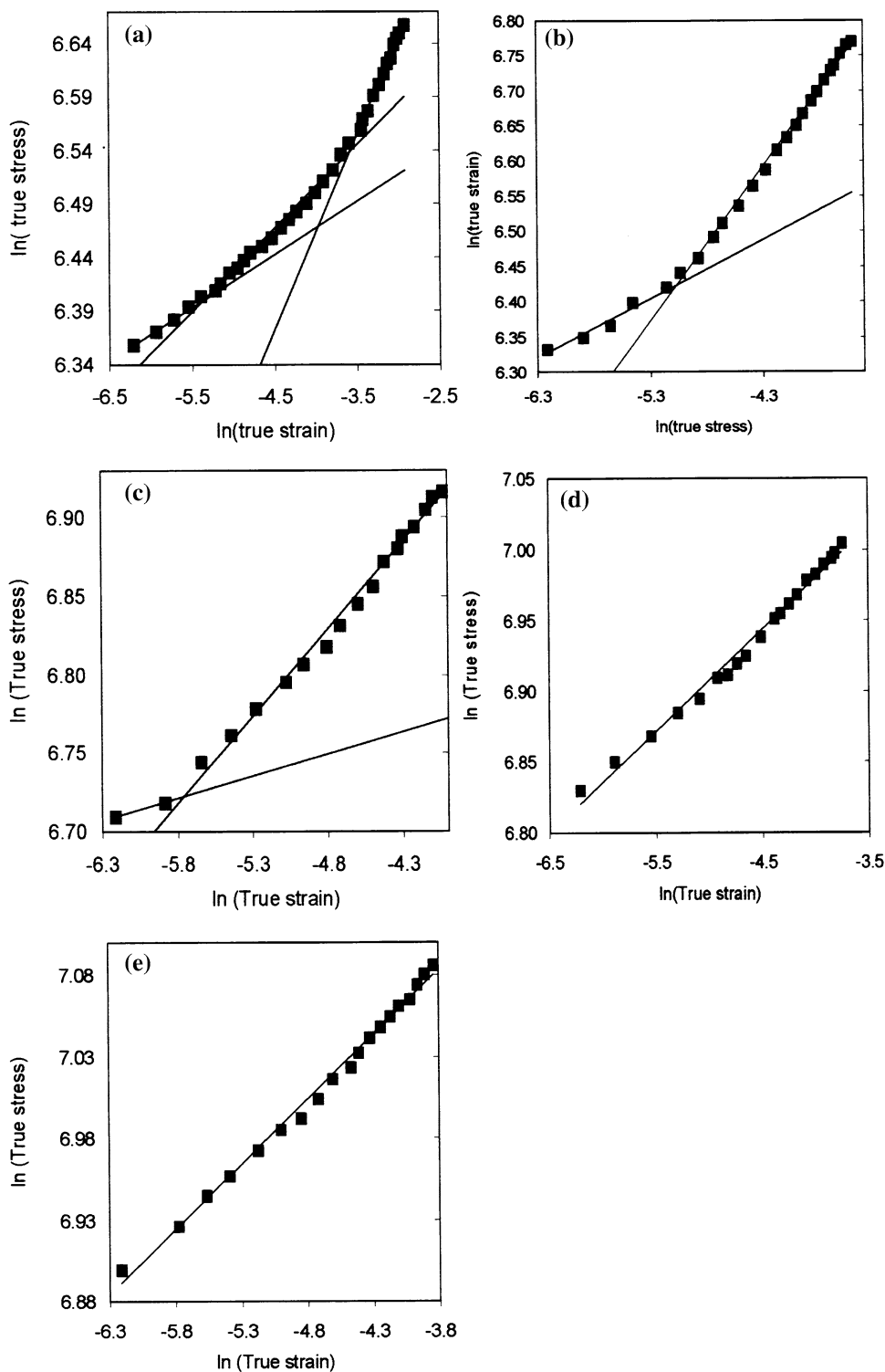


Fig. 13 Tensile properties of samples subjected to stepped austempering

Fig. 14 Strain-hardening behaviour of samples subjected to stepped austempering. First step times of (a) 10 min, (b) 20 min, (c) 30 min, (d) 45 min, and (e) 60 min

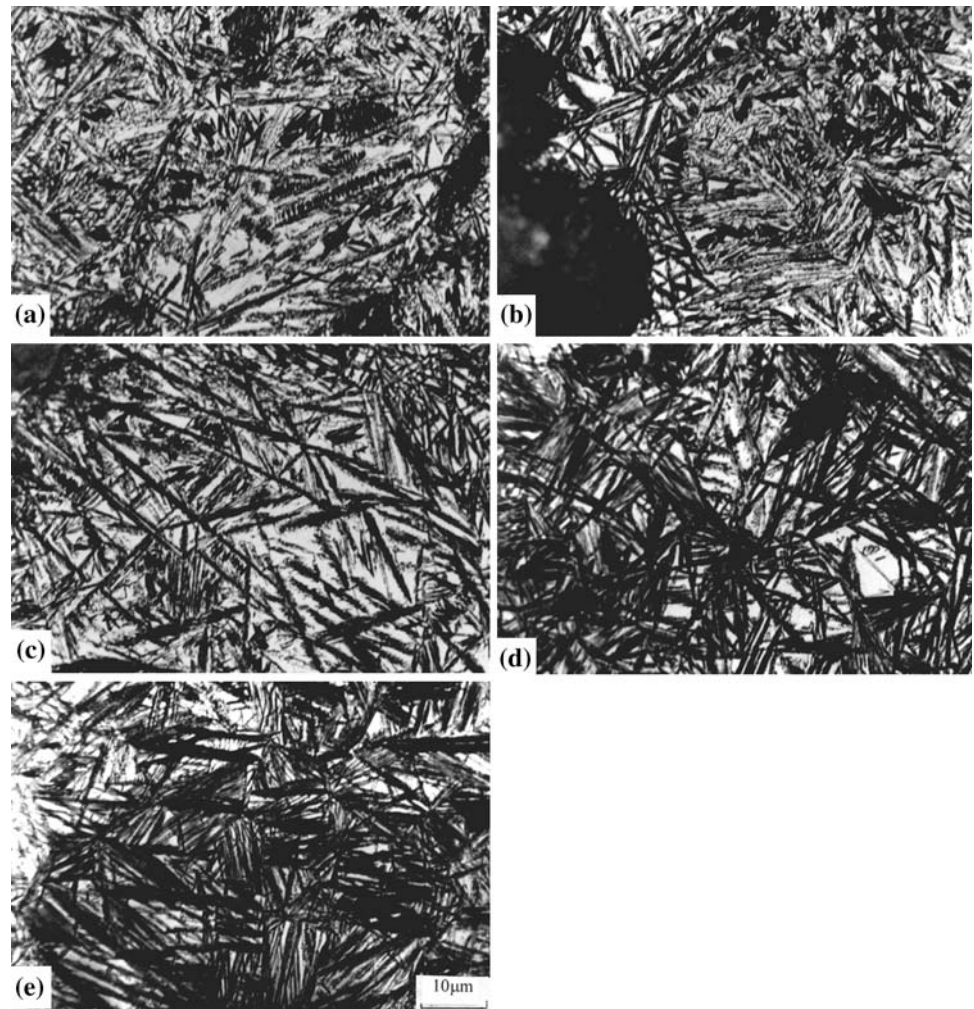


those austempered at 300 °C and 400 °C. This is to be expected since they have retained austenite content and its carbon content intermediate of those of the other two.

In order to confirm the strain dependence of martensite formation, a set of samples were austenitised at 950 °C and then austempered at 400 °C for 2 h. These were strained on

the Instron machine to different levels of 3, 5, 7 and 9%. The samples were unloaded after the above levels of strain, removed from the machine, and cut in the centre of the gauge length to study the microstructure. Optical microstructures are shown in Fig. 10. Increasing amount of martensite with increasing strain can be clearly observed.

Fig. 15 Microstructures of fracture surfaces of samples subjected to stepped austempering. First step times of (a) 10 min, (b) 20 min, (c) 30 min, (d) 45 min, and (e) 60 min



X-ray diffraction studies showed that the amount of retained austenite decreased with increasing strain as shown in Fig. 11. A set of typical diffraction profiles is shown in Fig. 12.

When subjected to stepped austempering, both the yield and tensile strengths were found to rise steadily as the first step time was increased as shown in Fig. 13. The strength increases with time primarily because of increasing volume fraction of lower ausferrite. As shown in the case of conventional austempering, the lower ausferrite is stronger than the upper ausferrite. As a result, the increasing volume fraction of the lower ausferrite in the microstructure results in increasing strength.

The strain-hardening behaviour of the samples subjected to stepped austempering revealed that, at short first step times, strain-hardening exponent was high, and the plot of stress against strain on log-log scale indicated change of slope. At longer first step times, the plot did not show any change of slope. A set of typical plots is shown in Fig. 14. As discussed earlier, a change of slope denotes change in

strain-hardening mechanism, and this involves formation of strain-induced martensite. Similar conclusions may be drawn in this case also. Thus, when the first step time is very short, formation of strain-induced martensite may be expected, while no martensite formation is to be expected when the first step time is long. This was observed to be so, through metallographic and X-ray diffraction studies. Figure 15 shows a set of microstructures of fractured samples which were subjected to stepped austempering. Martensite could be clearly observed in abundance in samples with first step times of 10 and 20 min. Much less of it was observed in samples with first step time of 30 min, and hardly any in those with first step times of 45 and 60 min. X-ray diffraction studies on the surface adjacent to the fracture surfaces revealed decreasing drop in retained austenite content as the first step time was increased, as shown in Fig. 16.

Studies with samples subjected to conventional austempering as well as those subjected to stepped austempering revealed considerable influence of the

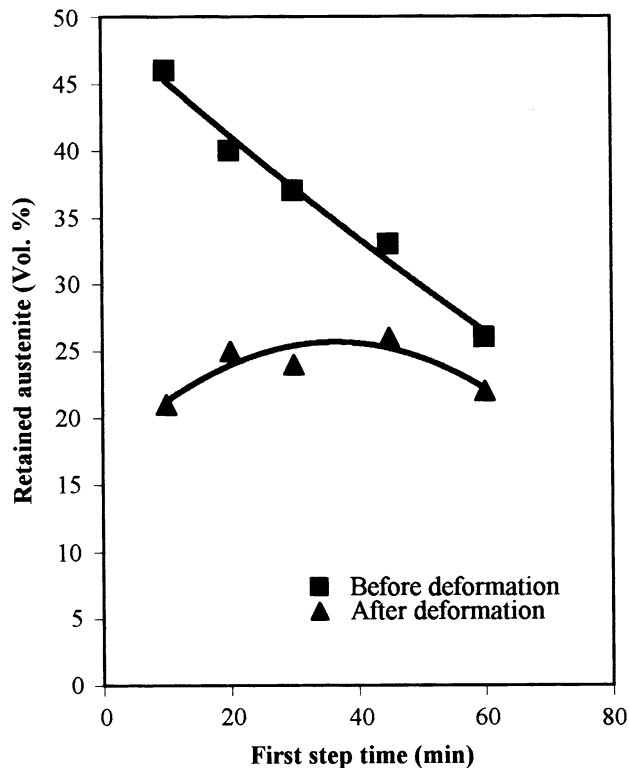


Fig. 16 Retained austenite content after deformation at different first step times

microstructure on the strain-induced transformation of austenite to martensite. While all of them contained considerable amount of retained austenite, they showed different tendency with regard to the formation of martensite on deformation. While the sample subjected to conventional austempering at 400 °C showed high tendency towards formation of strain-induced martensite, the sample subjected to conventional austempering at 300 °C, showed the least. The former showed all the attributes for low stability of austenite, such as coarse size, lower carbon content and blocky morphology. The samples austempered at 300 °C showed opposite features. In addition, these samples had fine ferrite laths in close proximity to austenite, which is believed to inhibit martensite formation. Samples austenitised at 350 °C exhibited microscopic features in between those of the above two, and exhibited intermediate tendency towards the formation of strain-induced martensite. Importance of the microstructural features detailed above is confirmed further when we examine the results of the samples subjected to stepped austempering. This shows a kind of composite microstructure, with upper and lower ausferrites as the two constituents. The tendency of these samples to generate strain-induced martensite depended on the relative amounts of the two constituents.

Conclusions

1. Samples subjected to austempering at higher temperatures have a greater tendency to produce strain-induced martensite.
2. This can be attributed to the larger size of the retained austenite in these samples.
3. At lower austempering temperatures, besides the fine size of the austenite, the presence of ferrite in large amount in close proximity to the austenite, also prevents formation of strain-induced martensite.
4. Stepped austempering results in a microstructure that is a mixture of lower and upper ausferrite.
5. The proportion of the two constituents depends on the first step time.
6. Samples subjected to short first step times, exhibit greater strain-hardening ability, due to the presence of larger amount of upper ausferrite.
7. Higher strain-hardening ability of ADI is due to strain-induced transformation of retained austenite.

Acknowledgement This work was financially supported by the Council of Scientific and Industrial Research, New Delhi, India.

References

1. Johansson M (1977) AFS Trans 85:117
2. Gundalach RB, Janowak JF (1983) AFS Trans 91:377
3. Rouns TN, Rundman KB, Moore DM (1984) AFS Trans 92:815
4. Gundalach RB, Janowak JF (1986) In: Proceedings of the 2nd International Conference on Austempered ductile iron, Ann Arbor, MI, USA, March. ASME Gear Research Institute, p 23
5. Aranzabal J, Gutierrez I, Rodriguez-Ibabe JM, Urcola JJ (1992) Mater Sci Technol 8:263
6. Timokhina IB, Hodgson PD, Pereloma EV (2004) Metall Mater Trans A 35A:2331
7. Tommita Y (1995) Mater Sci 30:105
8. Reisner G, Werner EA, Kerschbbaum P, Papst I, Fischer FD (1997) J Met 49(9):62
9. De Meyer M, Vanderschueren D, De Cooman BC (1999) Iron Steel Inst Jpn Int 39(8):813
10. Bai DQ, Di Chiro A, Yue S (1998) Mater Sci Forum 284–286:253
11. Chen HC, Era H, Shimizu M (1989) Metal Trans A 20A:437
12. Miihkinen VTT, Edmonds DV (1987) Mater Sci Technol 3:422
13. Takahashi M, Bhadeshia HKDH (1991) Mater Trans JIM 32:689
14. Wang J, Van Der Zwaag S (2001) Wire 50:1527
15. Tsukatani I, Hashimoto S, Inoue T (1991) Iron Steel Inst Jpn Int 31(9):992
16. Cullity BD (1974) Elements of x-ray diffraction. Addison-Wesley, Reading, MA, p 411
17. Roberts CS (1953) Trans AIME 197:203
18. Prasad Rao P, Putatunda SK (1998) Metall Mater Trans A 29A:3005
19. Rundman KB, Klug RC (1982) AFS Trans 90:499
20. Voigt RC, Loper CR (1984) In: Proceedings of the 1st International Conference on austempered ductile iron. ASM, Metals Park, OH, p 83
21. Hollomon TH (1945) Trans AIME 162:268